https://doi.org/10.5194/cp-2021-8
Preprint. Discussion started: 4 February 2021

Climate of the Past Discussions

Evolution of mean ocean temperature in Marine Isotope Stages 5-4

Sarah Shackleton[1*], James A. Menking[2], Edward Brook[2], Christo Buizert[2], Michael N. Dyonisius[3⊥], Vasilii V. Petrenko[3], Daniel Baggenstos[4], Jeffrey P. Severinghaus[1]

[1]Scripps Institution of Oceanography, University of California, San Diego, La Jolla, 92093, United States
[2]College of Earth, Ocean and Atmospheric Sciences, Oregon State University, Corvallis, 97331, United States
[3]Earth and Environmental Sciences, University of Rochester, Rochester, 14642, United States
[4]Climate and Environmental Physics, Physics Institute and Oeschger Centre for Climate Change Research, University of Bern, Bern, Switzerland
[*]Present address: Department of Geosciences, Princeton University, Princeton, 08544 United States
[⊥]Present address: Centre for Ice and Climate, Niels Bohr Institute, University of Copenhagen, Copenhagen, Denmark

Correspondence to: Sarah Shackleton (ss77@princeton.edu)

Abstract. Deglaciations are characterized by relatively fast and near-synchronous changes in ice sheet volume, ocean temperature, and atmospheric greenhouse gas concentrations, but glacial inceptions occur more gradually. Understanding the evolution of ice sheet, ocean, and atmospheric conditions from interglacial to glacial maximum provides important insight into the interplay of these components of our climate system. Using noble gas measurements in ancient ice samples, we reconstruct mean ocean temperature (MOT) from 74 to 59.5 ka BP, covering the Marine Isotope Stage (MIS) 5-4 boundary, MIS 4, and part of the MIS 4-3 transition. Comparing this MOT reconstruction to previously published MOT reconstructions from the last glacial cycle, we find that the majority of interglacial-glacial ocean cooling occurred across MIS 5, and MOT reached full glacial levels by MIS 4 (-2.7±0.3°C relative to the Holocene). Comparing MOT to contemporaneous records of CO_2 and benthic $\delta^{18}O$, we find that ocean cooling and the solubility pump can explain most of the CO_2 drawdown and increase in $\delta^{18}O$ across MIS 5. The timing of ocean warming and cooling in our record indicates that millennial scale climate variability plays a crucial role in setting mean ocean temperature during this interval, as seen during other periods, such as the last deglaciation.

1 Introduction

The classical view of Pleistocene glacial cycles is a slow build-up of ice sheets followed by rapid disintegration (Abe-ouchi et al., 2013; Emiliani, 1955; Hays et al., 1976; Imbrie et al., 1993). However, the long build-up of ice sheets over the last glacial cycle was punctuated by a rapid global cooling at the Marine Isotope Stage (MIS) 5a-4 boundary, at ~70 ka B.P. during the last glacial inception. During this period, roughly half of the interglacial-glacial drawdown of atmospheric CO_2 occurred in roughly four thousand years. This transition also brought extensive global cooling, build-up of polar ice sheets, and changes in deep ocean circulation (Adkins, 2013; Bereiter et al., 2012; Cutler et al., 2003; Yu et al., 2016). The mechanisms behind this rapid change are not yet fully understood.

https://doi.org/10.5194/cp-2021-8
Preprint. Discussion started: 4 February 2021


Climate of the Past Discussions

Multiple lines of oceanographic evidence (Adkins, 2013; Piotrowski, 2005; Thornalley et al., 2013; Yu et al., 2016) suggest that the MIS 5a-4 boundary marks the transition from the interglacial to glacial mode of ocean circulation. MIS 4 (like MIS 2) is characterized by cold conditions in both hemispheres and by the near absence of millennial scale variability (Fig. 1). Sea surface temperature records for MIS 4 and MIS 2 (Kohfeld and Chase, 2017; Snyder, 2016) indicate that globally, these two intervals were comparably cold, though the spatial distribution of temperature may have differed (Kohfeld and Chase, 2017). While similarities exist between the MIS 4 and MIS 2 intervals, there are notable differences. Northern Hemisphere ice sheets were not as extensive as they were during MIS 2 (Cutler et al., 2003), but MIS 4 conditions included greater glacial extent in New Zealand than during MIS 2, which may reflect greater ice extent in the Southern Hemisphere more broadly (Schaefer et al., 2015).

One powerful indicator of global climate is the mean ocean temperature (MOT), which can be reconstructed using atmospheric noble gas ratios in ice core trapped air (Headly and Severinghaus, 2007). The total inventory of krypton and xenon in the ocean-atmosphere system is fixed, and the portion of the total that is dissolved in the global oceans depends on the MOT, as solubility of these heavy noble gases is strongly temperature dependent (Ritz et al., 2011). Ice core Kr/N_2, Xe/N_2, and Xe/Kr reflect the fraction of the noble gas inventory not dissolved in the ocean, which allows MOT at that time to be reconstructed (Baggenstos et al., 2019; Bereiter et al., 2018a; Shackleton et al., 2019, 2020). Here we reconstruct MOT from 74 to 59.5 ka, covering the MIS 5a-4 transition, MIS 4, and part of the MIS 4-3 transition. The new record serves multiple purposes. First, it allows for a direct MIS 2 - MIS 4 comparison, to assess whether MIS 4 represents the full glacial oceanic mode. Second, comparison of MOT to benthic $\delta^{18}O$ changes from the onset of the Last Interglacial (MIS 5e) to MIS 4 and 2 provides insight into the temporal evolution of ocean temperature and ice volume changes over the glacial cycle. Third, superposed on the long-term global cooling trends leading up to the MIS 5-4 transition are Dansgaard-Oeschger (DO) cycles (Dansgaard et al., 1982), millennial-scale climate oscillations that are thought to be linked to mode changes in the Atlantic Meridional Overturning Circulation (AMOC) (Lynch-Stieglitz, 2017; Stocker and Johnsen, 2003). The link between the AMOC and ocean heat content has been observed in MOT reconstructions over the last two terminations (Baggenstos et al., 2019; Bereiter et al., 2018a; Shackleton et al., 2020), however the influences of millennial scale and glacial-interglacial climate change on MOT are difficult to disentangle. Our record allows us to better understand the millennial-scale controls on global ocean heat content outside of terminations. Last, we estimate the contribution of whole-ocean cooling to the decrease in atmospheric CO_2 across MIS 5 and the MIS 5a-4 boundary to examine the evolving controls on CO_2 through these intervals.

2 Methods

2.1 Site Description and Ice Core Measurements

Ice samples were obtained by drilling a shallow (20 m, 0.24 m diameter) ice core at Taylor Glacier, Antarctica, a blue ice area located in the McMurdo Dry Valleys (Baggenstos et al., 2017). The core contains ice spanning gas ages from ~58 ka near the surface to 74 ka at 20 meters depth (Menking et al., 2019). We excluded samples above 4 m depth to avoid

https://doi.org/10.5194/cp-2021-8
Preprint. Discussion started: 4 February 2021


Climate of the Past Discussions

alteration/contamination due to near-surface thermal fractures (Baggenstos et al., 2017). A total of 56 samples from Taylor Glacier were measured, including 10 replicate samples. In addition, four WAIS (West Antarctic Ice Sheet) Divide samples from MIS 4 were measured to replicate the Taylor Glacier results using samples from a different ice core. All ice core samples were analysed for Kr/N_2, Xe/N_2, and Xe/Kr using the method described by (Bereiter et al., 2018b). The average of the three noble gas ratios was used to determine the final MOT following procedures in (Shackleton et al., 2019). For brevity, we will refer to the MOT reconstructed from measured noble gases as 'MOT data' in this work.

2.2 Taylor Glacier Age Model

We apply the ice core age model of (Menking et al., 2019) with slight modifications for the MOT reconstruction. The age model was developed by matching measured variations in CH_4 and $\delta^{18}O_{atm}$ in the Taylor Glacier ice core to deep ice core records on the AICC2012 timescale (Veres et al., 2013). Tie points were manually selected, and noble gas sample ages were determined from linear interpolation between tie points. For this study, we selected tie points from the higher resolution NGRIP (rather than EDML) CH_4 record on AICC2012, plus three additional tie points from the EDML CO_2 record, also on AICC2012 (Table 1). Tie point uncertainties are reported relative to AICC2012, and do not include age uncertainty of the AICC2012 chronology itself. Tie point uncertainties have a minimal impact on the interpretation of the record.

2.3 Fractionation Corrections and Box Model Parameterizations

The noble gas ratios measured in ice cores must be corrected for fractionation that occurs within the firn, which alters the noble gas ratios from their original atmospheric values (Headly and Severinghaus, 2007). We apply the correction approach of (Shackleton et al., 2019), which uses a linear least-squares method to solve and correct for gravitational (Schwander, 1989) and thermal (Severinghaus et al., 1998) fractionations using measurements of isotope ratios of inert gases (whose atmospheric compositions do not measurably change over time). Argon isotope ratios were corrected for the gradual increase in atmospheric ^{40}Ar (Bender et al., 2008).

Fractionation corrections are more robust when calculating relative MOT change, rather than absolute MOT values, because errors in the fractionation corrections produce a systematic offset in the corrected noble gas ratios, whereas the relative changes in these ratios are minimally influenced ((Shackleton et al., 2020) and Appendix A). We therefore report MOT relative to Holocene MOT measured in the same ice core. For the Taylor Glacier samples, we compare our data to five early Holocene (10.6 ka) replicate Taylor Glacier samples from (Shackleton et al., 2020). WAIS Divide samples are reported relative to the average of Holocene samples from 11-10 ka (n=4) (Bereiter et al., 2018a). While the Taylor Glacier and WAIS Divide Holocene references are not from identical intervals, the WAIS Divide (Bereiter et al., 2018a) and EPICA Dome C (EDC) (Baggenstos et al., 2019) records both suggest that the entire Holocene was a very stable interval for MOT (1σ standard deviations of 0.2°C and 0.1°C respectively for all Holocene samples). For comparison of our MIS 4 MOT data to MIS 2, we consider published MOT data from the MIS 2 for Taylor Glacier (19.9 ka, five replicate samples) (Shackleton et al., 2020) and WAIS Divide (Bereiter et al., 2018a) (24-18 ka). In contrast to the Holocene, data from MIS 2 suggests that MOT was relatively

https://doi.org/10.5194/cp-2021-8
Preprint. Discussion started: 4 February 2021


Climate of the Past Discussions

variable during this interval (1σ standard deviations of 0.3°C and 0.5°C respectively for samples from 24-18 ka from WAIS Divide and EDC respectively), which somewhat complicates the comparison of MOT during the MIS 2 and MIS 4 intervals. Further details on the fractionation corrections applied are included in Appendix A.

We employ the box model of (Bereiter et al., 2018a), which calculates the MOT anomaly relative to the modern ocean from the atmospheric noble gas ratios. Parameterizations of the box model applied in this study are detailed in (Baggenstos et al., 2019). The box model requires input of sea level (Grant et al., 2012) to account for changes in the oceanic reservoir of xenon, krypton, and nitrogen that are unrelated to ocean temperature change. This includes changes in ocean volume, salinity, and sea surface pressure (Headly and Severinghaus, 2007). For Holocene MOT reference data and the MIS 2 data against which the record is compared, we use the sea level record of (Lambeck et al., 2014) in the box model. We also re-evaluate the WAIS Divide Holocene and MIS 2 MOT record (Bereiter et al., 2018a), applying the same box model parameterizations as applied in this study (and in (Shackleton et al., 2020)) for a consistent comparison.

2.4 Error Analysis

The error on our MOT reconstruction is estimated by propagating all known uncertainties using a Monte Carlo method. Sources of uncertainty include the analytical uncertainties for the noble gas ratios as well as the isotope ratios used for firn fractionation corrections. Additional uncertainties include the age uncertainty for the Taylor Glacier tie points (Table 1) and temporal and analytical uncertainties in the sea level curve.

We first created 10,000 versions of the dataset using a bootstrapping technique where the data were randomly varied within the uncertainties described above. We then fitted each time series using a spline with a 2500-year cut-off period and averaged the resulting splines to produce a final, smoothed version of our MOT record including uncertainty estimates.

3 Results

3.1 MIS 5a-4 Boundary

During the rapid drawdown in atmospheric CO_2 (72 - 68 ka, Fig. 2), we observe mean ocean cooling in two phases, with an overall net cooling of 0.9±0.3°C (1σ). In the first phase (72-70 ka) MOT decreased by 0.7±0.3°C in roughly two thousand years, coincident with Antarctic cooling and Greenland Interstadial 19. In the second phase (70-68 ka) MOT stabilized, then decreased further by 0.2±0.3°C, reaching a minimum at ~68 ka.

3.2 Comparison of MOT in MIS 4 and MIS 2

Our Taylor Glacier data show that MIS 4 MOT was statistically indistinguishable from MIS 2 (-0.1±0.3°C relative to MIS 2, or -2.7±0.3°C relative to the Holocene). The four WAIS Divide MOT data are consistent with the Taylor Glacier results (-2.6±0.5°C relative to the Holocene), but the WAIS data show more scatter. If we instead correct the WAIS Divide data for thermal fractionation using a firn model (Buizert et al., 2015) as in (Bereiter et al., 2018a) and compare the results to MIS 2

https://doi.org/10.5194/cp-2021-8
Preprint. Discussion started: 4 February 2021


Climate of the Past Discussions

125 data using this method of fractionation correction, we find that the WAIS Divide MIS4 data are slightly less scattered (Fig. 2). With these corrections applied, the MIS 4 interval in WAIS Divide is slightly warmer (-2.5±0.3°C relative to the Holocene). While all results are indistinguishable within error, these results emphasize the importance of future work developing further understanding of firn air processes and their influence on MOT results.

3.3 MIS 4-3 Transition

130 While our record may not capture the full transition into MIS 3, we find that there was substantial MOT warming at the end of MIS 4. By ~59.5 ka, MOT had reached levels comparable to the MIS 5a MOT peak at ~72 ka. Because our record does not contain a clear levelling of MOT, it is uncertain if or by how much MIS 3 MOT exceeded levels found at the end MIS 5a.

4 Discussion

135 ### 4.1 Ocean cooling and CO_2 drawdown across MIS 5a-4

We identify and discuss here two separate drawdowns of CO_2 during the glacial inception, each of which was approximately 40 ppm. The first occurred from MIS 5e to MIS 5a, the second from MIS 5a to MIS4. Using a carbon cycle box model ((Bauska et al., 2016), Appendix B) we estimate that the observed MOT net cooling of 0.9°C over the MIS 5a-4 transition would have led to a CO_2 drawdown of 9±3 ppm by solubility alone, which is a relatively small but not insignificant
140 fraction of the ~40 ppm drawdown that occurred over the full interval (Fig. 3). More information about the carbon box model applied in this study can be found in Appendix B.

A comparison of the Taylor Glacier records of MOT and CO_2 over the MIS 5a-4 transition shows that while MOT decreased more rapidly in the first half of the transition, the rate of decrease in CO_2 was relatively constant over the full transition. This observation is robust because both the CO_2 and MOT records are from the same ice archive, thus there is no
145 uncertainty in the relative timing of MOT and CO_2 variations. While ocean cooling may explain a considerable portion of the early CO_2 drawdown in the first half of the transition, the MOT and CO_2 trends clearly diverged around 70.5 ka.

It is notable that MOT was already low during MIS 5a (Fig. 3). Between the onset of MIS 5e and the end of MIS 5a, MOT had decreased by 3.1±0.4°C, for an estimated 32±4 of the ~40 ppm CO_2 lowering that occurred across MIS 5e to 5a. This is consistent with the hypothesis presented by (Adkins, 2013), that ocean solubility played a substantial role in setting
150 atmospheric CO_2 during MIS 5 but was not the main driver of the abrupt CO_2 decrease at the MIS 5a-4 boundary. Our data allows us to put tighter constraints on the role of the solubility pump in atmospheric CO_2 variations across these intervals. Out of the full 80 ppm CO_2 from MIS 5e to MIS 4, MOT changes can explain 41±4 ppm.

https://doi.org/10.5194/cp-2021-8
Preprint. Discussion started: 4 February 2021


Climate of the Past Discussions

4.2 MOT and benthic $\delta^{18}O$ during MIS 4

Benthic $\delta^{18}O$ records changes in seawater $\delta^{18}O$ and local deep-water temperature. We used the Taylor Glacier MOT record to estimate the temperature component of a global benthic $\delta^{18}O$ stack (Lisiecki and Stern, 2016) during MIS 4. Applying the benthic $\delta^{18}O$ temperature sensitivity of 0.26‰/°C at 3.5°C from (Shackleton, 1974), we find that the ocean temperature anomaly accounts for 0.7‰ of the 1.3‰ $\delta^{18}O$ anomaly relative to Holocene/modern benthic $\delta^{18}O$, implying the remaining 0.6‰ is due to enhanced ice sheet volume. For comparison, the MIS 2 - Holocene benthic $\delta^{18}O$ change is 1.7‰. Using a mean ice $\delta^{18}O$ of -30‰ and average ocean depth of 3790m (as in (Cutler et al., 2003)) the remaining 0.6‰ $\delta^{18}O$ anomaly would suggest a MIS 4 sea level anomaly of -71±10m. This finding is in reasonable agreement with the MIS 4 coral sea level benchmark of -81±1m (Cutler et al., 2003), and it is 30% higher than the average MIS 4 sea level used as our box model input (-94m, (Grant et al., 2012)) to calculate MOT from measured noble gas ratios. If we adjust the initial box model input so that MOT and sea level inputs are consistent with the decomposition of the benthic stack, our calculated MIS 4 MOT would be 0.1°C higher than the reported value, and the sea level then implied by the benthic stack (-75±10m) would be in closer agreement with the coral sea level benchmark.

This exercise demonstrates that the MOT result is robust to errors in the prescribed sea level; a one-meter error in sea level results in a 0.006°C error in MOT. Conversely, an error in the decomposition of the benthic stack results in a much larger error in ocean temperature. Every meter of sea level error in the benthic stack decomposition results in an 0.03°C error in ocean temperature, roughly five times the sensitivity found for our computation of MOT.

We note that there are distinct challenges in using MOT to decompose $\delta^{18}O$, as we have, such as the uncertainty in aligning sediment and ice core age scales. However, future comparisons of MOT, sea level, and benthic $\delta^{18}O$ records may provide valuable insight into disentangling sea level and ocean temperature information from benthic $\delta^{18}O$. For example, the observation that MIS 4 MOT is comparable to MIS 2 but sea level is ~50 m higher is consistent with previous findings that most of the interglacial to glacial ocean cooling occurs early in the glaciation and precedes substantial Northern Hemisphere ice sheet growth (Cutler et al., 2003; Shakun et al., 2015; Waelbroeck et al., 2002). This decoupling of ocean cooling and ice sheet growth may be an important clue for future investigation of the mechanism of glacial cycles.

4.3 MOT, Antarctic Temperature, and the Bipolar Seesaw

Records of the last two deglaciations have shown MOT increase and Antarctic warming during intervals of weakened AMOC, and Antarctic cooling and MOT decrease with AMOC recovery. Our new MOT record shows the same trend of Antarctic warming and MOT increase during Greenland Stadials 20 and 18, and Antarctic cooling and MOT decrease during Interstadial 19, suggesting that the interplay between AMOC, MOT and Antarctic temperature is a general feature of the climate system (Fig. 4). The same link between AMOC strength and MOT has been simulated in global climate models (Galbraith et al., 2016; Pedro et al., 2018), providing further confirmation of this phenomenon.

https://doi.org/10.5194/cp-2021-8
Preprint. Discussion started: 4 February 2021


Climate of the Past Discussions

Our MOT record shows a generally symmetric pattern of warming and subsequent cooling during Greenland Stadial 20 and Interstadial 19, suggesting that much of the 0.9°C cooling during the MIS 5a-4 transition may be related to millennial scale changes in the AMOC, rather than a more dramatic regime shift in ocean circulation suggested by other climate records during this interval (Adkins, 2013; Bereiter et al., 2012; Thornalley et al., 2013). However, the cooling during Interstadial 19 appears slightly more abrupt than the warming of Stadial 20. This stadial – interstadial transition occurs during a time of 65°N summer insolation minimum and substantial Northern Hemisphere ice sheet growth, which suggests that the slight asymmetry in MOT increase and decrease during this interval may be due to the superposition of the millennial scale AMOC variability on longer-term global cooling trends.

After the MIS 5a-4 transition, MOT, Antarctic and Greenland temperature remained low and stable during the long Greenland Stadial 19. Theories explaining the apparent lack of bipolar seesaw behaviour during very cold periods (such as MIS 4 and MIS 2) have invoked mechanisms related to thresholds in ice volume (McManus et al., 1999) and Southern Ocean temperature (Buizert and Schmittner, 2015). While ice volume during MIS 2 exceeds that of MIS 4, MOT during MIS 2 and MIS 4 indicate equally cold ocean conditions. This supports the idea that thresholds in ocean temperature, rather than global ice volume, may determine the presence or absence of millennial scale variability within a glacial.

4.4 Coevolution of MOT, Antarctic Temperature, CO2, and benthic $\delta^{18}O$

While the MOT proxy was developed over a decade ago (Headly and Severinghaus, 2007), only in the last few years have high resolution MOT records become available (Baggenstos et al., 2019; Bereiter et al., 2018a; Shackleton et al., 2019, 2020). With the additional data from this study, we take the opportunity to review the available MOT data and its relation to other key climate variables (Fig. 4).

As highlighted in this, and several other MOT studies (Bereiter et al., 2018a; Shackleton et al., 2019, 2020), one of the most striking features of the MOT records is their strong correlation to Antarctic water isotope records (Fig. 4a). It is remarkable that the MOT- δD scaling is similar on millennial and glacial-interglacial timescales, given that climate dynamics on these two timescales are likely to be different. Multiple explanations can be given for the strong correlation.

If there indeed is a causal relationship between MOT and Antarctic temperature, causality could plausibly run in either direction. First, it has been suggested that Southern Hemisphere high-latitude temperature, for which Antarctic δD is a proxy, provides a control on MOT (Bereiter et al., 2018a). Given that a large fraction of the global ocean interior is ventilated in the Southern Ocean (Johnson, 2008), processes acting in the Southern Ocean around Antarctica are likely to be important in setting the MOT. The temperature of deep waters formed in the Southern Ocean, as well as the rate at which they form, is probably linked to Southern Hemisphere high-latitude climate, providing a pathway to control MOT variations (Bereiter et al., 2018a). Additionally, the volume of cold dense brine formed on the Antarctic coast varies with the intensity of katabatic winds, which increase in a colder climate, providing another pathway for Antarctic climate to control bottom-water temperature and MOT (Talley et al., 2011).

https://doi.org/10.5194/cp-2021-8
Preprint. Discussion started: 4 February 2021


Climate of the Past Discussions

Second, it is possible that causality runs in the opposite direction, with MOT being a strong control on Antarctic δD. In their modelling study, (Pedro et al., 2018) proposed a mechanism linking MOT to Antarctic temperature on millennial timescales, as part of their effort to provide a more thorough dynamical framework for the bipolar seesaw. Briefly, during weakened AMOC intervals, ocean warming centred in the intermediate-depth North Atlantic is spread throughout the ocean basins via Kelvin and Rossby waves, which cannot cross the Antarctic Circumpolar Current. The enhanced temperature gradient across the Antarctic Circumpolar Current drives poleward ocean and atmospheric eddy heat fluxes, which are amplified by sea ice reduction and the ice-albedo feedback. The net result is a strong warming of the Antarctic continent. In this view, it is feasible that the MOT controls Antarctic temperature, via variations in Southern Ocean poleward eddy heat transport and sea ice feedbacks.

Last, MOT and Antarctic temperature need not be causally linked; the tight correlation between them may reflect a shared dependence on a third variable that is most likely AMOC variability. It is well established that Antarctic temperature responds to AMOC variations via the bipolar seesaw mechanism (Stocker and Johnsen, 2003). Likewise, AMOC variations and their associated changes in oceanic heat loss to the Arctic atmosphere, have been shown to influence MOT (Galbraith 2016, Pedro 2018). Thus, it is conceivable that both variables respond to AMOC variations without the necessity of a direct causal link between them.

Here we remain agnostic as to which of these three explanations is the correct one. Such a determination would require detailed modelling studies that are beyond the scope of the present work.

Next we address the relationship between CO_2 and MOT (Fig. 4b), which is likely quite dynamic in nature. Changes in the radiative forcing from atmospheric CO_2 changes influence top-of-atmosphere radiative imbalance, and thus ocean heat content. Such a link is well known from modern anthropogenic carbon emissions. In turn, ocean temperature affects solubility of CO_2 and thereby the partitioning of the carbon inventory between the ocean and atmosphere. The expected proportionality between MOT and atmospheric CO_2 due to this solubility effect is denoted by the gray arrow in Fig. 4b. As noted elsewhere (e.g. (Sigman et al., 2010)) the atmospheric CO_2 variations are larger than can be explained by ocean solubility alone.

Additionally, covariation of MOT and atmospheric CO_2 may be controlled by a third variable, such as changes in ocean circulation. It is likely that all three linkages are at play in the considered time intervals. As previously discussed, changes in ocean solubility across MIS 5 may account for a large portion of the CO_2 variability during this interval. However, MOT data within MIS 5 are sparse.

The link between ocean temperature and benthic foraminiferal $\delta^{18}O$ (Fig. 4c) has long been recognized (Emiliani, 1955; Shackleton, 1974). While MOT represents volume-averaged ocean temperature, the intermediate and deep ocean make up the majority of total ocean volume. The benthic $\delta^{18}O$ record (Lisiecki and Stern, 2016) shown in Fig. 1 and 3 contains stacked records from intermediate and deep sites, and (when binned into ocean regions) covers approximately 70% of the total ocean volume. Changes in MOT should therefore be largely reflected in temperature-driven changes in this $\delta^{18}O$ record. The scaling between MOT and $\delta^{18}O$ for ocean temperature change at 3.5°C (Holocene/modern MOT, or ΔMOT=0) from (Shackleton, 1974) is denoted by the grey arrow in Fig. 4c. While the temperature dependence of $\delta^{18}O$ from (Shackleton, 1974)

https://doi.org/10.5194/cp-2021-8
Preprint. Discussion started: 4 February 2021


Climate of the Past Discussions

is quadratic, it is essentially linear in the temperature range of the plotted MOT data (i.e. $d\delta^{18}O/dT$ varies by less than 6% in the ΔMOT range shown in Fig. 4).

The other primary control on benthic $\delta^{18}O$ is ice volume. Considering the temporal evolution of $\delta^{18}O$ and MOT, it is possible to gain insight into the relative controls on $\delta^{18}O$ during the intervals where $\delta^{18}O$ and MOT data are available. For example, considering the MOT-$\delta^{18}O$ relationship for late MIS5a/MIS 4 (light green), late MIS 3 (cyan) and MIS 2 (light blue), there is some variability in MOT within these intervals, but average MOT across the intervals remains essentially unchanged. However, there is a clear long-term evolution of $\delta^{18}O$ across these intervals. This suggests (consistent with previous studies (Adkins, 2013; Cutler et al., 2003; Shakun et al., 2015)) that the long-term trend in $\delta^{18}O$ after the MIS 5-4 transition is primarily driven by changes in global ice volume. As previously discussed, improvement in linking the ice core and sediment core timescales will enable further insight into extracting ocean temperature and ice volume information from $\delta^{18}O$ with MOT reconstructions.

5 Conclusions and Future Outlook

Our record clearly demonstrates that ocean cooling during the MIS 5a-4 transition can only explain a small (~9 ppm) fraction of the concomitant ~40 ppm drop in atmospheric CO_2; however, MOT changes can explain a relatively large fraction (~32 ppm) of the ~40 ppm drop in atmospheric CO_2 from MIS 5e to MIS 5a.

Mean ocean cooling at the MIS 5-4 transition was fully reversed at the MIS 4-3 transition, suggesting no net change in the solubility pump from the end of MIS 5 to the onset of MIS 3 despite a ~20-ppm difference in atmospheric CO_2. The ocean had already cooled by more than 3°C between MIS 5e and MIS 5a, which can explain most of the net CO_2 change over this interval. MOT records spanning the full MIS 5 interval would provide further insight into the control of ocean temperature on CO_2 variability during the early stages of glacial inception.

Our record provides the first observational evidence that MOT responds to AMOC changes outside of deglaciations and shows bipolar seesaw-like behaviour during Greenland Stadial 20 and Interstadial 19. As during MIS 2, MOT was low and stable during MIS 4, which may suggest that stable glacial ocean conditions occur when oceans cool below a certain threshold. However, we cannot completely preclude other similarly cold times during the glacial period without additional data.

Studies comparing the CO_2 (Bereiter et al., 2012) and Atlantic Western Boundary Undercurrent (Thornalley et al., 2013) response to millennial scale variability during MIS 5 and 3 suggest that the changes in ocean circulation at the MIS 5-4 boundary altered the nature of abrupt climate change between these two intervals. Comparison of the MOT response to DO cycles within MIS 5 and 3 may provide further insight into the differences between these intervals.

This study demonstrates that it is possible to capture MOT changes during the larger of the millennial-scale DO events using the noble gas ratio technique. However, comparison of the MOT records between smaller DO events will push the current analytical limits of this method. While improvements in analytical precision will benefit future studies, a fuller understanding

https://doi.org/10.5194/cp-2021-8
Preprint. Discussion started: 4 February 2021


Climate of the Past Discussions

of gas fractionation processes within the ice and firn, and the mechanisms of air-sea gas exchange will be critical to accurate interpretation of ice core MOT records.

285

6 Appendix A: Comparison of MOT results using different methods of fractionation corrections and between Kr/N_2, Xe/N_2, and Xe/Kr

Gases are trapped in bubbles in ice during the process of firnification, as snow compacts and densifies into firn and 290 eventually glacial ice. This process is gradual, occurring on timescales on the order of hundreds to thousands of years. During this time, the low permeability of the firn restricts bulk air motion but allows for air in the open pores to exchange with the overlying atmosphere and throughout the firn column primarily through molecular diffusion. This mechanism of air transport allows for processes such as gravitational settling (Schwander, 1989), thermal diffusion (Severinghaus et al., 1998), and kinetic fractionation (Birner et al., 2018; Buizert and Severinghaus, 2016; Kawamura et al., 2013) to alter Kr/N_2, Xe/N_2 and Xe/Kr 295 from their atmospheric compositions before bubble close-off. Correction of Kr/N_2, Xe/N_2 and Xe/Kr for these processes may be done with output from a firn model, and/or from measurements of inert gas isotope ratios, which are also influenced by these processes but are unchanging in the atmosphere. As stated in the main text, argon isotope ratios are the slight exception, due to the degassing ^{40}Ar from the solid earth (Bender et al., 2008). With the known rate of change in atmospheric ^{40}Ar and age of the samples, a small (<0.005‰) correction is applied to measured $\delta^{40/38}Ar$ and $\delta^{40/36}Ar$.

300 Figure A1 shows the MIS 4 Taylor Glacier MOT data (average of the Kr/N_2, Xe/N_2 and Xe/Kr results) with fractionation corrections for gravitational fractionation, gravitational and thermal fractionation, and gravitational and kinetic fractionation (Shackleton et al., 2020). For a detailed explanation of these methods of fractionation correction, see the supporting information of (Shackleton et al., 2020). In this study, as in (Shackleton et al., 2019), the corrections for gravitational and thermal fractionation are chosen over the other described methods. The reason for this choice is that 1) it 305 gives the best agreement in Taylor Glacier MOT results between replicate samples for the Holocene and MIS 2 (Shackleton et al., 2020), and 2) it gives the best results for calculated MOT in firn air and surface ice samples from a wide range of site conditions (Shackleton, 2019). Results are compared between these differing methods of fractionation correction when i) they are not calculated relative to a reference interval, ii) they are calculated relative to Holocene MOT, and iii) they are calculated relative to MIS 2 MOT. As previously shown, MOT reported relative to a reference interval in the same core is more robust 310 to the method of fractionation correction than when no reference interval is used (Shackleton et al., 2020). However, even when the MIS 4 MOT data are referenced to Holocene MOT, there appears to be a small, but systematic offset in the MOT results using different methods of fractionation correction. If the MIS 4 data are calculated relative to data relative to MIS 2 from the same ice core, the offset is reduced.

Comparison of the MOT results from Kr/N_2, Xe/N_2 and Xe/Kr when normalized to Holocene versus MIS 2 MOT 315 data show a similar phenomenon to the observed offset in results between differing fractionation corrections (Fig. A2). The offset between the MOT results for the three noble gas ratios is present, regardless of the fractionation correction applied; if

https://doi.org/10.5194/cp-2021-8
Preprint. Discussion started: 4 February 2021


Climate of the Past Discussions

the MOT results from the individual ratios are reported relative to those from the Holocene, there is a small offset between the MOT results from Kr/N_2, Xe/N_2 and Xe/Kr. However, if the MOT difference is calculated between MIS 2 and our MIS 4 data, the offset diminishes.

The observed patterns are consistent with systematic uncertainties in the fractionation corrections applied to the noble gas ratios. Differences in site conditions, such as temperature, accumulation, and atmospheric circulation can lead to differences in firn column height, temperature profile, and dynamics of gas transport and mixing within the firn. These have implications for gravitational, thermal, and kinetic fractionation of Kr/N_2, Xe/N_2, and Xe/Kr. While the fractionation corrections should account and correct for these changes, a systematic error in these corrections, or the presence of an additional fractionating process that has not been accounted for, may result in systematic error that varies with site condition. This would result in a similar magnitude of systematic error under similar firn conditions. Thus, the systematic differences in MOT results using different fractionation correction methods, or between the three noble gas ratios are largest when comparing results between glacial and interglacial intervals but are minimal when comparing MOT results between the MIS 4 and MIS 2 glacial intervals.

However, a systematic error in fractionation correction may not be the only explanation for the offset in MOT results between Kr/N_2, Xe/N_2 and Xe/Kr. Processes that decouple atmospheric noble gas exchange from ocean heat exchange may also introduce systematic error in MOT reconstructions, and may affect the krypton, xenon and nitrogen to different degrees, resulting in differences in MOT reconstructed from Kr/N_2, Xe/N_2 and Xe/Kr. If this were the cause of the observed offset in MOT results between the three noble gas ratios, we would predict that the offset would be consistent between ice cores.

Considering the MIS 4, MIS 2, and Holocene data from the WAIS Divide record, the relatively sparse and somewhat noisier data make it difficult to discern any trends. However, if anything, the relative offset in the three noble gas proxies is opposite of that observed for Taylor Glacier. This suggests that the primary mechanism to explain the observed differences in the MOT results between Kr/N_2, Xe/N_2 and Xe/Kr is a process that affects these ratios within the firn or ice, rather than the atmospheric inventories of Xe, Kr, and N_2. However, this does not rule out the existence of processes related to the latter. While the slight differences in results with different fractionation correction and between the 3 noble gas ratios do not affect the conclusions of the study, further investigation is necessary to gain a better grasp on these processes' influence on the MOT proxies and their associated uncertainties.

7 Appendix B: Ocean Solubility Effect on CO_2

To estimate the effect of a cooling ocean on atmospheric CO_2 concentration, we used a box model (Bauska et al., 2016) to run a forward scenario of prescribed ocean temperature change between MIS 5e and MIS 4. The model consists of fourteen boxes representing the surface oceans (six boxes), intermediate oceans (two boxes), and deep oceans (three boxes), a well-mixed atmosphere (one box), and a terrestrial biosphere (two boxes). The model simulates thermohaline circulation and

https://doi.org/10.5194/cp-2021-8
Preprint. Discussion started: 4 February 2021


Climate of the Past Discussions

mixing, air-sea gas exchange, export production, sediment burial/ $CaCO_3$ compensation, and exchange of carbon between the atmosphere and terrestrial biosphere.

The timing and relative magnitudes of ocean cooling were prescribed to the surface ocean boxes by linearly scaling surface ocean temperatures to variations in the EPICA Dome C δD record (Jouzel et al., 2007) (Fig. 3). The δD record was first corrected for changes in seawater δD using the $\delta^{18}O$ seawater reconstruction of (Waelbroeck et al., 2002) and 8:1 scaling of δD:^{18}O changes. The absolute magnitude of cooling from MIS 5e-4 was chosen such that MOT decreased by 3.1 °C between MIS 5e-5a and by 0.9 °C across the MIS 5a-4 transition, consistent with ice core MOT data ((Shackleton et al., 2020) and this study). The relative change in global mean ocean surface temperature (MOST) that we prescribed to the model closely matches relative changes in a stack of 136 sediment core records (Kohfeld and Chase, 2017) (Fig. 3)

Whole ocean salinity change was also prescribed in the model to account for the solubility effect on CO_2. Salinity was linearly scaled to the sea level record from the Red Sea (Grant et al., 2014) assuming a pre-industrial salinity of 34.72 p.s.u. and a Last Glacial Maximum salinity of 35.85 p.s.u. (Adkins et al., 2002).

The total modelled CO_2 drawdown due to salinity and MOT changes between MIS 5e-4 was 41 ppm (Fig. 3). The drawdown between MIS5e-MIS 5a was larger (-32 ppm), while the MIS 5-4 transition showed less of an effect (-9 ppm). Our results represent a plausible estimate of the magnitude of solubility-induced CO_2 drawdown between MIS 5e-4 that is consistent with the ice core MOT data (Shackleton et al., 2020), however the estimate could likely be improved using more complex models of the carbon cycle.

Data availability

Data presented in this study are available online at https://doi.org/10.15784/601415.

Author contributions

JPS, EB, and VVP designed the research. SS performed the noble gas measurements. JAM constructed the age model. SS ran the MOT box model simulations. JAM ran carbon box model simulations. CB ran the WAIS Divide firn model simulations. MND led field logistics for Taylor Glacier sample acquisition. SS, JAM, MND and DB analysed the data. SS wrote the paper with input from all authors.

Competing interests

The authors declare that they have no conflict of interest.

Acknowledgements

We thank Mike Jayred for drilling the core analysed in this study and Kathy Schroeder for managing the Taylor Glacier field camp. Thanks to Thomas Bauska, Rachael Rhodes, Peter Sperlich, Isaac Vimont, Jake Ward, Heidi Roop, Peter Neff, Joe McConnell, Bernhard Bereiter, and Andrew Smith for their help with field logistics, drilling, and sampling of ice cores. Ice

https://doi.org/10.5194/cp-2021-8
Preprint. Discussion started: 4 February 2021

Drilling Design and Operations (IDDO) provided drilling support, and the US Antarctic Program provided logistical support for this project. Thanks to Michael Bender for providing helpful feedback on early drafts of this paper. This research was supported by NSF grants 1246148 (SIO), 1245821 (OSU) and 1245659 (UR). This material is based upon work supported by the National Science foundation Graduate Research Fellowship under Grant No. DGE-1650112.

References

Abe-ouchi, A., Saito, F., Kawamura, K., Raymo, M. E., Okuno, J., Takahashi, K. and Blatter, H.: Insolation-driven 100,000-year glacial cycles and hysteresis of ice-sheet volume, Nature, 500(7461), 190–193, doi:10.1038/nature12374, 2013.

Adkins, J. F.: The role of deep ocean circulation in setting glacial climates, Paleoceanography, 28, 1–23, doi:10.1002/palo.20046, 2013.

Adkins, J. F., Mcintyre, K. and Schrag, D. P.: The Salinity, Temperature, and d18O of the Glacial Deep Ocean, Science, 298, 1769–1773, doi:10.1126/science.1076252, 2002.

Andersen, K. K., Azuma, N., Barnola, J. M., Bigler, M., Biscaye, P., Caillon, N., Chappellaz, J., Clausen, H. B., Dahl-Jensen, D., Fischer, H., Flückiger, J., Fritzsche, D., Fujii, Y., Goto-Azuma, K., Grønvold, K., Gundestrup, N. S., Hansson, M., Huber, C., Hvidberg, C. S., Johnsen, S. J., Jonsell, U., Jouzel, J., Kipfstuhl, S., Landais, A., Leuenberger, M., Lorrain, R., Masson-Delmotte, V., Miller, H., Motoyama, H., Narita, H., Popp, T., Rasmussen, S. O., Raynaud, D., Rothlisberger, R., Ruth, U., Samyn, D., Schwander, J., Shoji, H., Siggard-Andersen, M. L., Steffensen, J. P., Stocker, T., Sveinbjörnsdóttir, A. E., Svensson, A., Takata, M., Tison, J. L., Thorsteinsson, T., Watanabe, O., Wilhelms, F. and White, J. W. C.: High-resolution record of Northern Hemisphere climate extending into the last interglacial period, Nature, 431(7005), 147–151, doi:10.1038/nature02805, 2004.

Baggenstos, D., Bauska, T. K., Severinghaus, J. P., Lee, J. E., Schaefer, H., Buizert, C., Brook, E. J., Shackleton, S. and Petrenko, V. V: Atmospheric gas records from Taylor Glacier, Antarctica, reveal ancient ice with ages spanning the entire last glacial cycle, Clim. Past, 13(7), 943–958, doi:10.5194/cp-13-943-2017, 2017.

Baggenstos, D., Häberli, M., Schmitt, J., Shackleton, S. A., Birner, B., Severinghaus, J. P., Kellerhals, T. and Fischer, H.: Earth's radiative imbalance from the Last Glacial Maximum to the present, Proc. Natl. Acad. Sci. U. S. A., 116(30), 14881–14886, doi:10.1073/pnas.1905447116, 2019.

Baumgartner, M., Kindler, P., Eicher, O., Floch, G., Schilt, A., Schwander, J., Spahni, R., Capron, E., Chappellaz, J., Leuenberger, M., Fischer, H. and Stocker, T. F.: NGRIP CH4 concentration from 120 to 10 kyr before present and its relation to a δ15N temperature reconstruction from the same ice core, Clim. Past, 10(2), 903–920, doi:10.5194/cp-10-903-2014, 2014.

Bauska, T. K., Baggenstos, D., Brook, E. J., Mix, A. C., Marcott, S. A., Petrenko, V. V., Schaefer, H., Severinghaus, J. P., Lee, J. E. and Thiemens, M. H.: Carbon isotopes characterize rapid changes in atmospheric carbon dioxide during the last deglaciation, Proc. Natl. Acad. Sci. U. S. A., 113(13), 3465–3470, doi:10.1073/pnas.1513868113, 2016.

Bender, M. L., Barnett, B., Dreyfus, G., Jouzel, J. and Porcelli, D.: The contemporary degassing rate of 40Ar from the solid Earth, Proc. Natl. Acad. Sci. U. S. A., 105(24), 8232–8237, doi:10.1073/pnas.0711679105, 2008.

Bereiter, B., Lüthi, D., Siegrist, M., Schüpbach, S., Stocker, T. F. and Fischer, H.: Mode change of millennial CO2 variability during the last glacial cycle associated with a bipolar marine carbon seesaw, Proc. Natl. Acad. Sci. U. S. A., 109(25), 9755–9760, doi:10.1073/pnas.1204069109, 2012.

Bereiter, B., Eggleston, S., Schmitt, J., Nehrbass-ahles, C., Stocker, T. F., Fischer, H., Kipfstuhl, S. and Chappellaz, J.: Revision of the EPICA Dome C CO2 record from 800 to 600 kyr before present, Geophys. Res. Lett., 47, 542–549, doi:10.1002/2014GL061957, 2015.

Bereiter, B., Shackleton, S., Baggenstos, D., Kawamura, K. and Severinghaus, J.: Mean global ocean temperatures during the last glacial transition, Nature, 553(7686), 39–44, doi:10.1038/nature25152, 2018a.

Bereiter, B., Kawamura, K. and Severinghaus, J. P.: New methods for measuring atmospheric heavy noble gas isotope and elemental ratios in ice core samples, Rapid Commun. Mass Spectrom., 32(10), 801–814, doi:10.1002/rcm.8099, 2018b.

Birner, B., Buizert, C., Wagner, T. J. W. and Severinghaus, J. P.: The influence of layering and barometric pumping on firn air transport in a 2-D model, Cryosphere, 12(6), 2021–2037, doi:10.5194/tc-12-2021-2018, 2018.

https://doi.org/10.5194/cp-2021-8
Preprint. Discussion started: 4 February 2021

Buizert, C. and Schmittner, A.: Southern Ocean control of glacial AMOC stability and Dansgaard-Oeschger interstadial duration, Paleoceanography, 30(12), 1595–1612, doi:10.1002/2015PA002795, 2015.
Buizert, C. and Severinghaus, J. P.: Dispersion in deep polar firn driven by synoptic-scale surface pressure variability, Cryosphere, doi:10.5194/tc-10-2099-2016, 2016.
Buizert, C., Cuffey, K. M., Severinghaus, J. P., Baggenstos, D., Fudge, T. J., Steig, E. J., Markle, B. R., Winstrup, M., Rhodes, R. H., Brook, E. J., Sowers, T. A., Clow, G. D., Cheng, H., Edwards, R. L., Sigl, M., McConnell, J. R. and Taylor, K. C.: The WAIS Divide deep ice core WD2014 chronology – Part 1: Methane synchronization (68-31 ka BP) and the gas age-ice age difference, Clim. Past, 11(2), 153–173, doi:10.5194/cp-11-153-2015, 2015.
Capron, E., Landais, A., Lemieux-Dudon, B., Schilt, A., Masson-Delmotte, V., Buiron, D., Chappellaz, J., Dahl-Jensen, D., Johnsen, S., Leuenberger, M., Loulergue, L. and Oerter, H.: Synchronising EDML and NorthGRIP ice cores using δ18O of atmospheric oxygen (δ18Oatm) and CH4 measurements over MIS5 (80-123 kyr), Quat. Sci. Rev., 29(1–2), 222–234, doi:10.1016/j.quascirev.2009.07.014, 2010.
Cutler, K. B., Edwards, R. L., Taylor, F. W., Cheng, H., Adkins, J., Gallup, C. D., Cutler, P. M., Burr, G. S. and Bloom, A. L.: Rapid sea-level fall and deep-ocean temperature change since the last interglacial period, Earth Planet. Sci. Lett., 206, 253–271, doi:10.1016/S0012-821X(02)01107-X, 2003.
Dansgaard, W., Clausen, H. B., Gundestrup, N., Hammer, C. U., Johnsen, S. F., Kristinsdottir, P. M. and Reeh, N.: A new Greenland deep ice core, Science, doi:10.1126/science.218.4579.1273, 1982.
Emiliani, C.: Pleistocene Temperatures, J. Geol., 63(6), 538–578, doi:10.1086/626295, 1955.
Galbraith, E. D., Merlis, T. M. and Palter, J. B.: Destabilization of glacial climate by the radiative impact of Atlantic Meridional Overturning Circulation disruptions, Geophys. Res. Lett., 43(15), 8214–8221, doi:10.1002/2016GL069846, 2016.
Grant, K. M., Rohling, E. J., Bar-Matthews, M., Ayalon, A., Medina-Elizalde, M., Ramsey, C. B., Satow, C. and Roberts, A. P.: Rapid coupling between ice volume and polar temperature over the past 150,000 years, Nature, 491(7426), 744–747, doi:10.1038/nature11593, 2012.
Grant, K. M., Rohling, E. J., Ramsey, C. B., Cheng, H., Edwards, R. L., Florindo, F., Heslop, D., Marra, F., Roberts, A. P., Tamisiea, M. E. and Williams, F.: Sea-level variability over five glacial cycles, Nat. Commun., 5(5076), 1–9, doi:10.1080/08989575.2017.1289316, 2014.
Hays, J. D., Imbrie, J. and Shackleton, N. J.: Variations in the Earth's Orbit: Pacemaker of the Ice Ages, Science, 194(4270), 1121–1132, doi:10.1126/science.194.4270.1121, 1976.
Headly, M. A. and Severinghaus, J. P.: A method to measure Kr/N2 ratios in air bubbles trapped in ice cores and its application in reconstructing past mean ocean temperature, J. Geophys. Res., 112(19), 1–12, doi:10.1029/2006JD008317, 2007.
Imbrie, J., Berger, A., Boyle, E. A., Clemens, S. C., Duffy, A., Howard, W. R., Kukla, G., Kutzbach, J., Martinson, D. G., McIntyre, A., Mix, A. C., Molfino, B., Morley, J. J., Peterson, L. C., Pisias, N. G., Prell, W. L., Raymo, M. E., Shackleton, N. J. and Toggweiler, J. R.: On the structure and origin of major glaciation cycles 2. The 100,000-year cycle, Paleoceanography, 8(6), 699–735, doi:10.1029/93PA02751, 1993.
Johnson, G. C.: Quantifying Antarctic Bottom Water and North Atlantic Deep Water volumes, J. Geophys. Res., 113(C5), C05027, doi:10.1029/2007JC004477, 2008.
Jouzel, J., Masson-Delmotte, V., Cattani, O., Dreyfus, G., Falourd, S., Hoffmann, G., Minster, B., Nouet, J., Barnola, J. M., Chappellaz, J., Fischer, H., Gallet, J. C., Johnsen, S., Leuenberger, M., Loulergue, L., Luethi, D., Oerter, H., Parrenin, F., Raisbeck, G., Raynaud, D., Schilt, A., Schwander, J., Selmo, E., Souchez, R., Spahni, R., Stauffer, B., Steffensen, J. P., Stenni, B., Stocker, T. F., Tison, J. L., Werner, M. and Wolff, E. W.: Orbital and Millennial Antarctic Climate Variability over the Past 800,000 years, Science, 317(5839), 793–796, doi:10.1126/science.1141038, 2007.
Kawamura, K., Severinghaus, J. P., Albert, M. R., Courville, Z. R., Fahnestock, M. A., Scambos, T., Shields, E. and Shuman, C. A.: Kinetic fractionation of gases by deep air convection in polar firn, Atmos. Chem. Phys., doi:10.5194/acp-13-11141-2013, 2013.
Kohfeld, K. E. and Chase, Z.: Temporal evolution of mechanisms controlling ocean carbon uptake during the last glacial cycle, Earth Planet. Sci. Lett., 472, 206–215, doi:10.1016/j.epsl.2017.05.015, 2017.
Lambeck, K., Rouby, H., Purcell, A., Sun, Y. and Sambridge, M.: Sea level and global ice volumes from the Last Glacial Maximum to the Holocene, Proc. Natl. Acad. Sci., 111(43), 15296–15303, doi:10.1073/pnas.1411762111, 2014.
Lisiecki, L. E. and Raymo, M. E.: A Pliocene-Pleistocene stack of 57 globally distributed benthic δ 18O records, Paleoceanography, 20(1), 1–17, doi:10.1029/2004PA001071, 2005.

https://doi.org/10.5194/cp-2021-8
Preprint. Discussion started: 4 February 2021

Lisiecki, L. E. and Stern, J. V.: Regional and global benthic δ 18 O stacks for the last glacial cycle, Paleoceanography, 31(10), 1368–1394, doi:10.1002/2016PA003002, 2016.
Lynch-Stieglitz, J.: The Atlantic Meridional Overturning Circulation and Abrupt Climate Change, Ann. Rev. Mar. Sci., doi:10.1146/annurev-marine-010816-060415, 2017.
McManus, J. F., Oppo, D. W. and Cullen, J. L.: A 0.5-Million-year record of millennial-scale climate variability in the North Atlantic, Science, 283(5404), 971–975, doi:10.1126/science.283.5404.971, 1999.
Menking, J. A., Brook, E. J., Shackleton, S. A., Severinghaus, J. P., Dyonisius, M. N., Petrenko, V., McConnell, J. R., Rhodes, R. H., Bauska, T. K., Baggenstos, D., Marcott, S. and Barker, S.: Spatial pattern of accumulation at Taylor Dome during Marine Isotope Stage 4: stratigraphic constraints from Taylor Glacier, Clim. Past, 15(4), 1537–1556, doi:10.5194/cp-15-1537-2019, 2019.
Pedro, J. B., Jochum, M., Buizert, C., He, F., Barker, S. and Rasmussen, S. O.: Beyond the bipolar seesaw: Toward a process understanding of interhemispheric coupling, Quat. Sci. Rev., 192, 27–46, doi:10.1016/j.quascirev.2018.05.005, 2018.
Piotrowski, A. M.: Temporal Relationships of Carbon Cycling and Ocean Circulation at Glacial Boundaries, Science, 307(5717), 1933–1938, doi:10.1126/science.1104883, 2005.
Ritz, S. P., Stocker, T. F. and Severinghaus, J. P.: Noble gases as proxies of mean ocean temperature: Sensitivity studies using a climate model of reduced complexity, Quat. Sci. Rev., 30(25–26), 3728–3741, doi:10.1016/j.quascirev.2011.09.021, 2011.
Schaefer, J. M., Putnam, A. E., Denton, G. H., Kaplan, M. R., Birkel, S., Doughty, A. M., Kelley, S., Barrell, D. J. A., Finkel, R. C., Winckler, G., Anderson, R. F., Ninneman, U. S., Barker, S., Schwartz, R., Andersen, B. G. and Schluechter, C.: The Southern Glacial Maximum 65,000 years ago and its Unfinished Termination, Quat. Sci. Rev., 114, 52–60, doi:10.1016/j.quascirev.2015.02.009, 2015.
Schwander, J.: The transformation of snow to ice and the occlusion of gases, Environ. Rec. Glaciers Ice Sheets, 53–67, 1989.
Severinghaus, J. P., Sowers, T., Brook, E. J., Alley, R. B. and Bender, M. L.: Timing of abrupt climate change at the end of the younger dryas interval from thermally fractionated gases in polar ice, Nature, 391(6663), 141–146, doi:10.1038/34346, 1998.
Shackleton, N. J.: Attainment of isotopic equilibrium between ocean water and the benthonic foraminifera geuns *Uvigerina*: Isotopic changes in the ocean during the last glacial, Colloq. Int. du C.N.R.S., 219, 203–210, 1974.
Shackleton, S.: Tracking Past Changes in Ocean Heat Content with Atmospheric Noble Gases in Ice Cores, PhD thesis, University of California San Diego., 2019.
Shackleton, S., Bereiter, B., Baggenstos, D., Bauska, T. K., Brook, E. J., Marcott, S. A. and Severinghaus, J. P.: Is the Noble Gas-Based Rate of Ocean Warming During the Younger Dryas Overestimated?, Geophys. Res. Lett., 46(11), 5928–5936, doi:10.1029/2019GL082971, 2019.
Shackleton, S., Baggenstos, D., Menking, J. A., Dyonisius, M. N., Bereiter, B., Bauska, T. K., Rhodes, R. H., Brook, E. J., Petrenko, V. V., McConnell, J. R., Kellerhals, T., Häberli, M., Schmitt, J., Fischer, H. and Severinghaus, J. P.: Global ocean heat content in the Last Interglacial, Nat. Geosci., 13(1), 77–81, doi:10.1038/s41561-019-0498-0, 2020.
Shakun, J. D., Lea, D. W., Lisiecki, L. E. and Raymo, M. E.: An 800-kyr record of global surface ocean δ18O and implications for ice volume-temperature coupling, Earth Planet. Sci. Lett., 426, 58–68, doi:10.1016/j.epsl.2015.05.042, 2015.
Sigman, D. M., Hain, M. P. and Haug, G. H.: The polar ocean and glacial cycles in atmospheric CO2 concentration, Nature, 466(7302), 47–55, doi:10.1038/nature09149, 2010.
Snyder, C. W.: Evolution of global temperature over the past two million years, Nature, 538(7624), 226–228, doi:10.1038/nature19798, 2016.
Stocker, T. F. and Johnsen, S. J.: A minimum thermodynamic model for the bipolar seesaw, Paleoceanography, 18(4), doi:10.1029/2003PA000920, 2003.
Talley, L. D., Pickard, G. L., Emery, W. J. and Swift, J. H.: Descriptive physical oceanography: An introduction., 2011.
Thornalley, D. J. R., Barker, S., Becker, J., Hall, I. R. and Knorr, G.: Abrupt changes in deep Atlantic circulation during the transition to full glacial conditions, Paleoceanography, 28, 253–262, doi:10.1002/palo.20025, 2013.
Veres, D., Bazin, L., Landais, A., Toye Mahamadou, K. H., Lemieux-Dudon, B., Parrenin, F., Martinerie, P., Blayo, E., Blunier, T., Capron, E., Chappellaz, J., Rasmussen, S. O., Severi, M., Svensson, A., Vinther, B. M. and Wolff, E. W.: The Antarctic ice core chronology (AICC2012): an optimized for the last 120 thousand years, Clim. Past, 9, 1733–1748, doi:10.5194/cp-9-1733-2013, 2013.
Waelbroeck, C., Labeyrie, L., Michel, E., Duplessy, J. C., Mcmanus, J. F., Lambeck, K., Balbon, E. and Labracherie, M.: Sea-

https://doi.org/10.5194/cp-2021-8
Preprint. Discussion started: 4 February 2021

level and deep water temperature changes derived from benthic foraminifera isotopic records, Quat. Sci. Rev., 21, 295–305, doi:10.1016/S0277-3791(01)00101-9, 2002.
Yu, J., Menviel, L., Jin, Z. D., Thornalley, D. J. R., Barker, S., Marino, G., Rohling, E. J., Cai, Y., Zhang, F., Wang, X., Dai, Y., Chen, P. and Broecker, W. S.: Sequestration of carbon in the deep Atlantic Sequestration of carbon in the deep during the last glaciation Atlantic during the last glaciation, Nat. Geosci., 2657, doi:10.1038/NGEO2657, 2016.

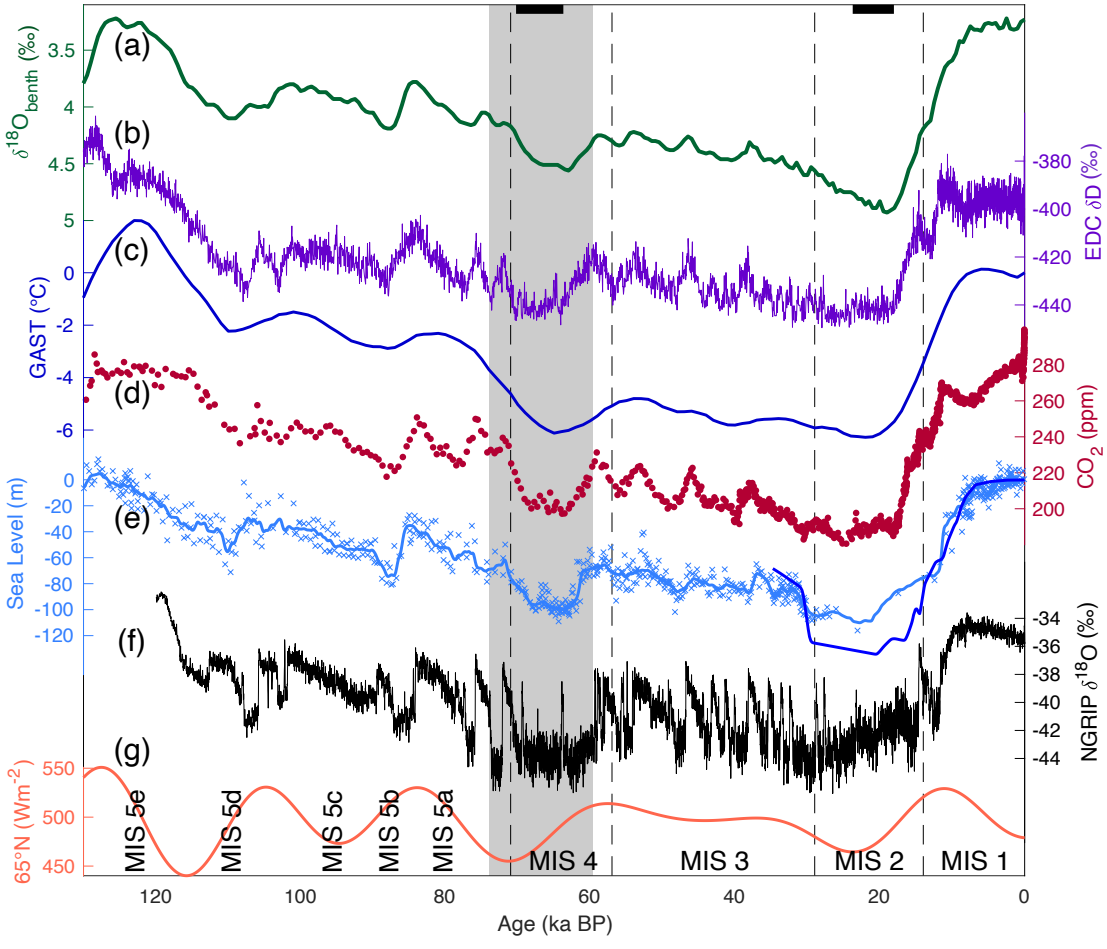

Figure 1: Climate records of the last glacial cycle. (a) Global benthic $\delta^{18}O$ stack (Lisiecki and Stern, 2016), (b) EDC δD (Jouzel et al., 2007), (c) global average surface temperature anomaly from present (Snyder, 2016), (d) CO_2 composite record (Bereiter et al., 2015), (e) relative (light blue) (Grant et al., 2012) and eustatic (royal blue) (Lambeck et al., 2014) sea level, (f) NGRIP $\delta^{18}O$ (Andersen et al., 2004), and (g) summer solstice insolation at 65°N. Dashed lines show boundaries between Marine Isotope Stages (MIS) from (Lisiecki and Raymo, 2005). Gray panel shows interval of the mean ocean temperature (MOT) record presented in this study. Black bars at top of figure show the intervals used to define MIS 4 (this study) and MIS 2 (Bereiter et al., 2018a) MOT.

https://doi.org/10.5194/cp-2021-8
Preprint. Discussion started: 4 February 2021

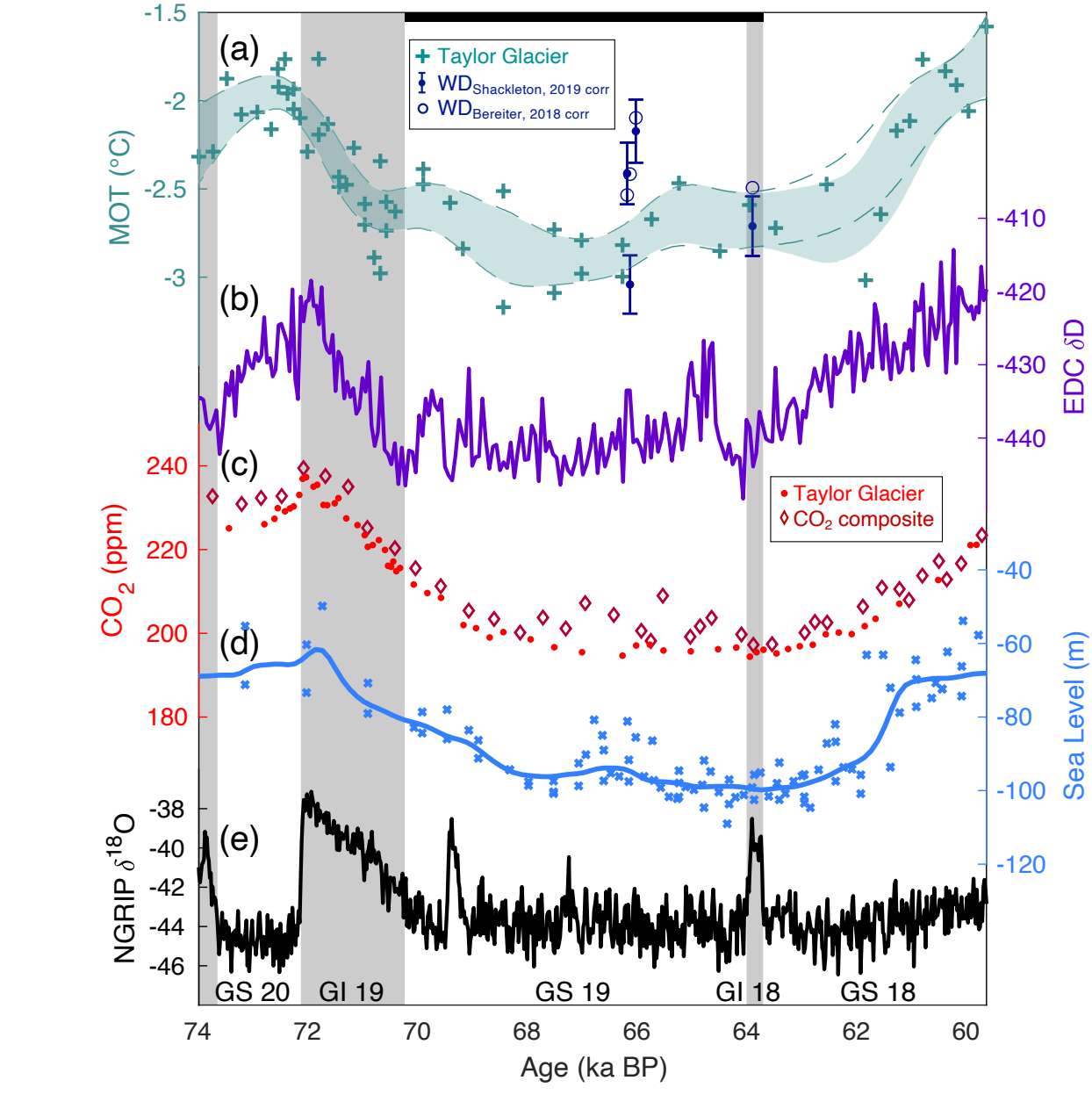

Figure 2: Mean Ocean Temperature (MOT) anomalies relative to the Holocene versus key climate variables. Panel (a) shows MOT data from Taylor Glacier (turquoise) and WAIS Divide (blue). Crosses indicate individual Taylor Glacier MOT data and shading shows 1σ confidence envelope of the Taylor Glacier data from a spline with a 2500-year cutoff period and bootstrapping. Dashed line shows the boundaries of the 1σ confidence envelope if the low MOT point at ~62 ka is not included. Solid blue points show WAIS Divide data corrected as described in the methods (with 1σ error bars) and open circles show the MOT results if the firn corrections detailed in (Bereiter et al., 2018a) are applied. (b) EDC δD (Jouzel et al., 2007) corrected for changes in seawater δD (see Appendix B), (c) CO_2 from EDML (diamonds) (Bereiter et al., 2012) and Taylor Glacier (points) (Menking et al., 2019) on AICC2012. (d) Relative sea level record (Grant et al., 2012), (e) NGRIP $\delta^{18}O_{ice}$ (Andersen et al., 2004) on AICC2012. Gray panels show warm Greenland intervals (interstadials) and white panels indicate cold Greenland intervals (stadials). Black bar at top of figure shows the time interval used to calculate Marine Isotope Stage 4 MOT.

https://doi.org/10.5194/cp-2021-8
Preprint. Discussion started: 4 February 2021

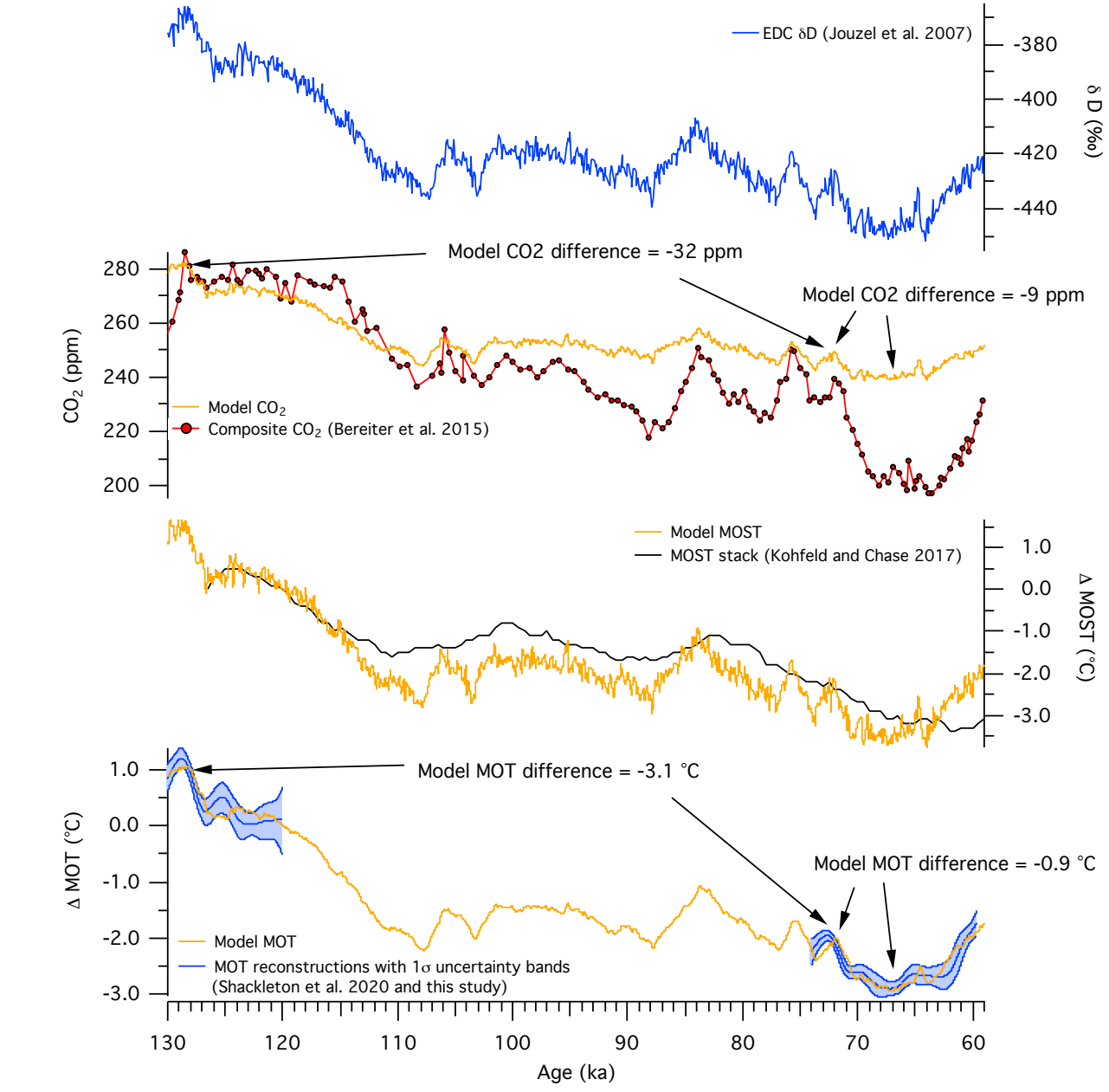

Figure 3: Results from a box model estimating the magnitude of CO_2 drawdown due to mean ocean temperature cooling. Inputs to the box model sea surface temperature changes (MOST, orange trace, panel 3) are scaled to ice core δD data corrected for seawater δD changes (blue trace, top panel). The sea surface temperature changes are transmitted to the deep ocean via circulation and mixing in the model, causing the mean ocean temperature (MOT, orange trace, panel 4) to evolve through time. The modelled MOT history agrees well with the existing (but limited) ice core MOT data (blue traces, panel 4). Ocean salinity also evolves in the model and is scaled to sea level data (Appendix B). The evolution of CO_2 in the model (orange trace, panel 2) is only due to changes in ocean solubility. The modelled CO_2 history is compared to ice core CO_2 records (red markers) (Bereiter et al., 2015). The modelled evolution of atmospheric CO_2 more closely resembles the ice core data for the MIS 5e-5c interval, suggesting that much of the CO_2 change during that time can be explained by ocean solubility changes alone. The changes after ~100 ka are more dramatic and must involve other processes such as changes in the marine biological pump, ocean circulation, or the amount of carbon stored on land.

https://doi.org/10.5194/cp-2021-8
Preprint. Discussion started: 4 February 2021

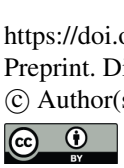

Climate of the Past Discussions
Open Access
EGU

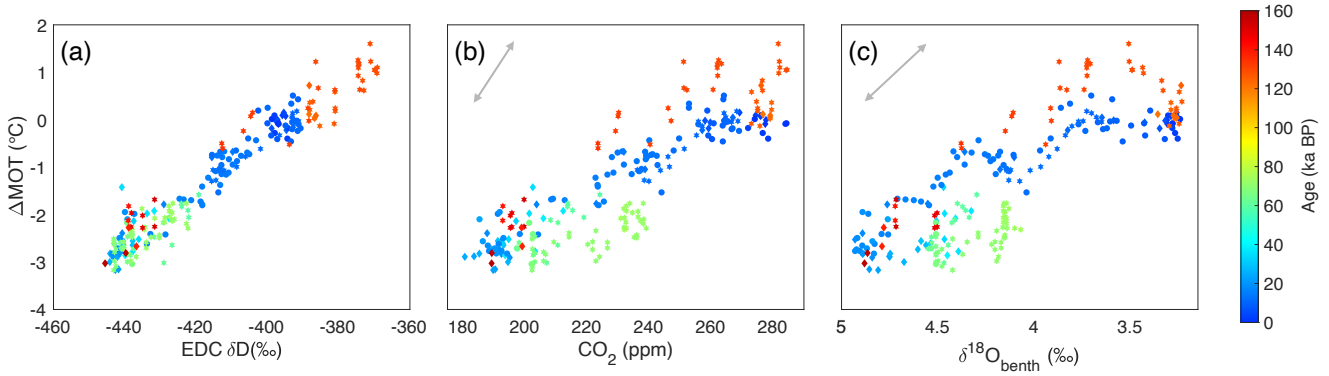

565

Figure 4: ΔMOT plotted against coeval (a) EDC δD (Jouzel et al., 2007) corrected for changes in seawater δD, (b) atmospheric CO_2 (Bereiter et al., 2015), and (c) $\delta^{18}O_{benth}$ (Lisiecki and Stern, 2016). The EDC ΔT, CO_2, and $\delta^{18}O_{benth}$ records were linearly interpolated in order to plot against contemporaneous MOT. Additionally, the EDC ΔT was smoothed using a gaussian filter with a 500-year window to remove high frequency variability. Gray arrow in (b) shows ΔMOT-CO_2 relationship for the solubility pump from the carbon box model. Gray arrow in (c) shows the ΔMOT- $\delta^{18}O$ scaling from (Shackleton, 1974). Diamonds indicate MOT data constructed from the EDC record (Baggenstos et al., 2019; Shackleton et al., 2020), circles show data from WAIS Divide (Bereiter et al., 2018a)(and this study), and stars show MOT data from Taylor Glacier (Shackleton et al., 2019, 2020)(and this study). Color of data indicate the age.

570

Gas Age (ka BP)	Depth (m)	Age_{min} (ka BP)	Age_{max} (ka BP)	Data	Source
59.02	3.15	58.7	59.2	CH_4	NGRIP
59.77	4.19	59.68	59.97	CH_4	NGRIP
60.45	5.125	59.8	62.5	CO_2	EDML
63.72	7.2	62.6	64.18	CO_2	EDML
64.2	7.79	63.86	64.5	CH_4	NGRIP
70.35	11.5	69.2	70.94	CO_2	EDML
71	13.25	70.43	71.95	CH_4	NGRIP
72.34	16.2	72.15	72.64	CH_4	NGRIP
72.7	17.4	72.2	73.3	$\delta^{18}O_{atm}$	NGRIP
73.74	19.27	73.35	74.5	$\delta^{18}O_{atm}$	NGRIP

575 **Table 1: Tie points used in this study.** Taylor Glacier CH_4, $\delta^{18}O_{atm}$, and CO_2 measurements are tied to pre-existing records of CH_4 (Baumgartner et al., 2014), $\delta^{18}O_{atm}$ (Capron et al., 2010), and CO_2 (Bereiter et al., 2012) from well-dated ice cores on the AICC2012 (Veres et al., 2013) chronology.

https://doi.org/10.5194/cp-2021-8
Preprint. Discussion started: 4 February 2021

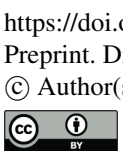

Climate of the Past Discussions
Open Access
EGU

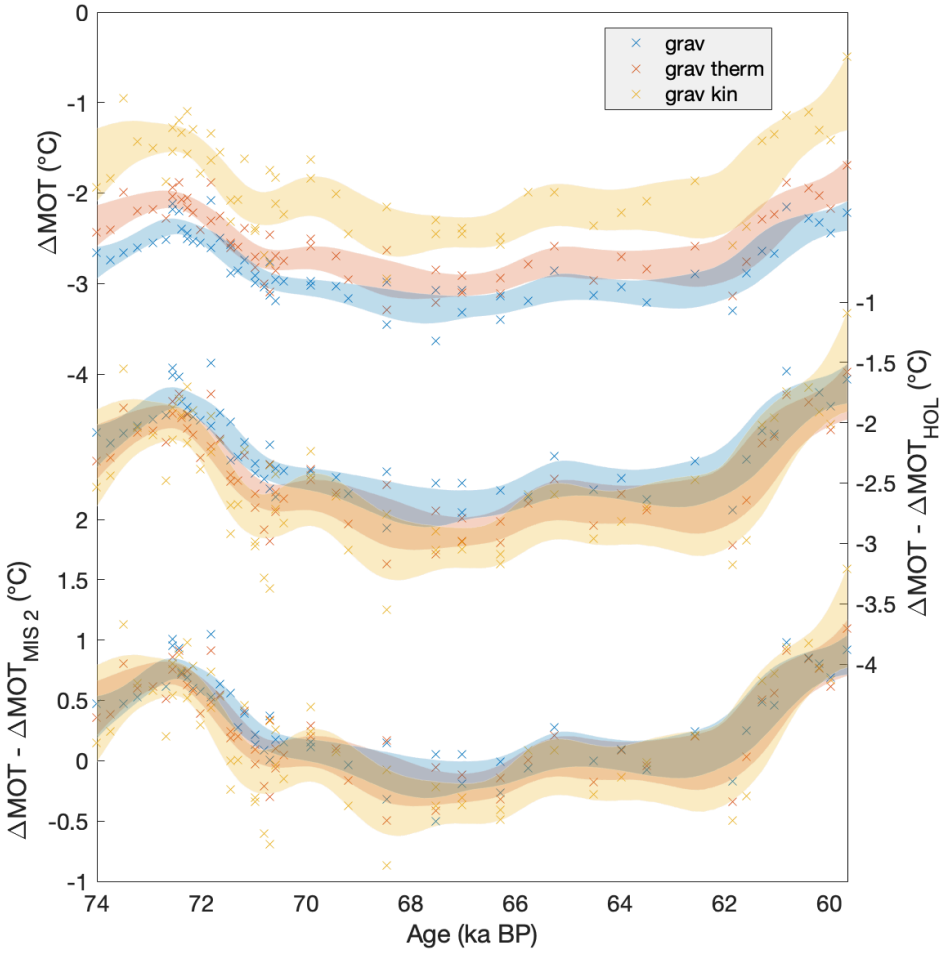

Figure A1: Comparison of mean ocean temperature (MOT) anomalies between three methods of fractionation correction. Results are for the average of the three MOT proxies (Kr/N_2, Xe/N_2 and Xe/Kr). The top panel shows results if the noble gas ratios are corrected for fractionation, and no reference interval is used. The middle panel shows the results when the noble gas ratios reported relative to Holocene data, using the same method of fractionation correction. The bottom panel is the same as the middle, but MOT is reported relative to MIS 2. Individual MOT data are shown with x's and the 1σ confidence envelope from a spline with a 2500 year cutoff period.

https://doi.org/10.5194/cp-2021-8
Preprint. Discussion started: 4 February 2021

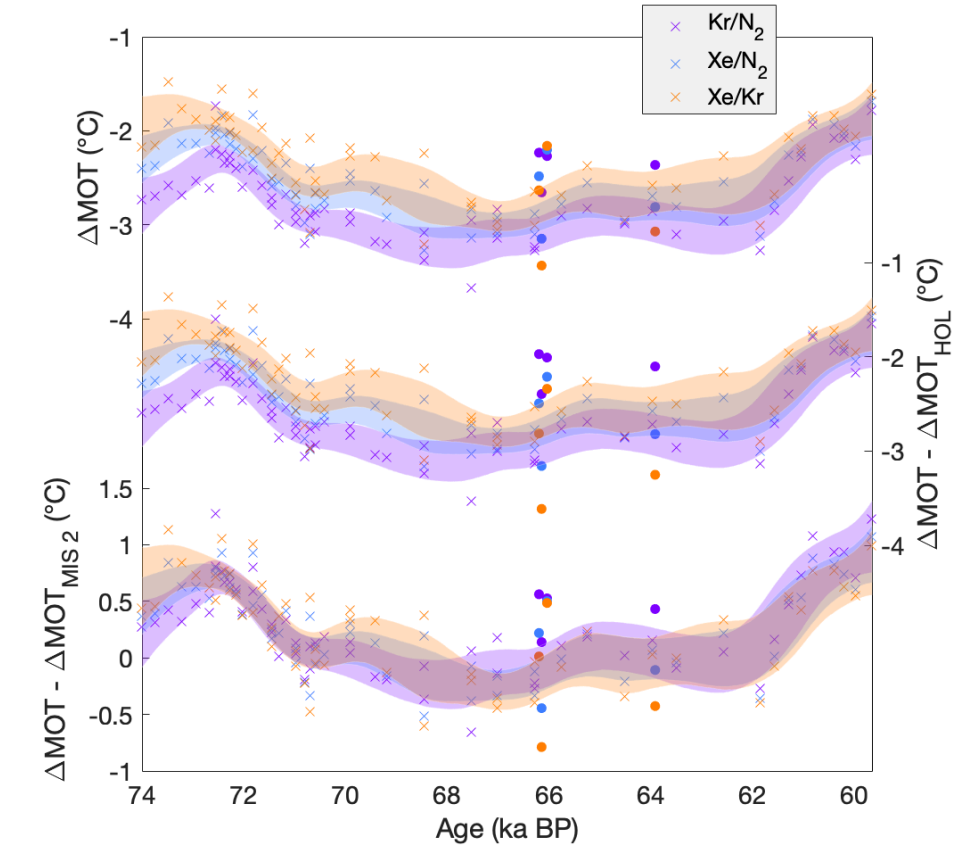

585 **Figure A2: Mean ocean temperature (MOT) anomalies calculated from Kr/N_2, Xe/N_2, and Xe/Kr.** Noble gas ratios are corrected for gravitational and thermal fractionation ((Shackleton et al., 2019) and this study). The top panel shows calculated MOT when no reference interval is used. The middle panel shows the MOT anomaly relative to Holocene MOT results from the three noble gas ratios. The bottom panel shows the MOT anomaly relative to MIS 2. Individual MOT data from Taylor Glacier are shown with x's and the 1σ confidence envelope from a spline with a 2500 year cutoff period is shown in shading. WAIS Divide data are shown as points.

590